Kinetics of Metal Ion Binding by Polysaccharide Colloids

Elise Rotureau* and Herman P. van Leeuwen

Laboratory of Physical Chemistry and Colloid Science, Wageningen University, Dreijenplein 6, 6703 HB Wageningen, The Netherlands

Received: January 17, 2008; Revised Manuscript Received: March 26, 2008

The dynamics of metal sorption by a gel-like polysaccharide is investigated by means of the electrochemical technique of stripping chronopotentiometry (SCP). The measured response reflects the diffusive flux properties of the metallic species in the dispersion. The colloidal ligand studied here is a functionalized carboxymethyldextran. Its complexation with Pb(II) reveals a time dependence that identifies strong differences in the dynamic nature of the successive metal complexes formed. Apparently, the formation of intramolecular bidentate complexes requires a slow conformational reorganization of the macromolecule that becomes the rate-limiting step in the complexation reaction. The relevant parameters for metal binding and release kinetics are computed and thus provide knowledge of the time-dependent stability and lability of metal polysaccharide complexes.

1. Introduction

The physicochemical surface and volume properties of colloids in natural waters are intimately related to their hydrodynamic features (size, shape and porosity etc.), as well as to their electrostatic features due to the presence of charges and metal ion-binding sites.[1,2] Most of the so-called soft colloids, such as polysaccharides,[3–5] generally carry negative charges and are permeable to both water and trace pollutants; consequently they are able to complex, immobilize and release metal ions.[2,6] The dynamic speciation and bioavailability of metal ions in such colloidal systems are closely linked and are strongly dependent on the nature of the particles involved. The broad diversity of available colloids gives rise to a large variety of metal complexes in a wide range of stabilities and labilities.[7] Electrochemical techniques such as voltammetry have been widely applied in the analysis of metal complexation mechanisms[8] and in the study of metal speciation in natural waters. Their flux-based response provides both thermodynamic and dynamic information on the system.[9] For example, stripping chronopotentiometry (SCP) measures the lability of metal complexes of latex particles functionalized with surface carboxyl groups, which confirms recently developed theory for complexation by colloidal ligands.[10–12] A decrease of signal upon addition of colloidal ligands to a metal ion solution generally arises from reduction of the average diffusion coefficient of the labile metal species and/or loss of lability of the colloidal metal complexes. Still, even in the presence of these effects, the shift of the characteristic potential allows the determination of the stability constant for 1:1 metal complexes in colloidal dispersions.[13] For complexation of heavy metals with soft polysaccharide particles, only few voltammetric studies are available so far. They mainly cover the evaluation of stability constants of the 1:1 complexes of alginate, polygalacturonic acid, pectin or carrageenan[14–16] or the 1:2 complexes of pectins.[17] Indeed, there is a paucity of information and understanding on the dynamic features of metal complexation by "soft" colloids and related aspects of the nature and stoichiometry of the macromolecular/polyelectrolytic complex. However, the macromolecular structural aspects of complexation between polysaccharides and metal ions have been the subject of a large number of studies. In general, the findings show the diversity of conformational changes[18,19] and the importance of the degree of chain stiffness. Natural colloids are generally difficult to define in terms of size, charge distribution, nature and composition, and this is especially true for carbohydrate compounds. The study of their properties requires the use of model polysaccharides such as alginic acid, dextran, succinoglycan, etc. In the present study, we chose carboxymethyldextran (CMD) as a model colloidal ligand. It was well defined in a previous study,[20] in which the complex interplay between electrostatic and hydrodynamic properties was underlined. The charged polymer CMD is an appropriate model system for the investigation of the interactions between soft permeable particles and metal ions for given conditions of pH and ionic strength. In this work, we discuss and analyze the binding of Pb(II) by several types of CMD, taking into account the impact of metal ion binding on the size of the CMD entity. The SCP data on Pb(II)/CMD reveal a typical time-dependence of the complexation that was not observed in the case of hard-particle complexing agents (carboxylated latex nanospheres). The decrease of the signal with time, upon addition of the colloidal ligand to the metal solution, identifies strong differences in the lability of the successive metal complexes formed. Here we will describe our findings and propose an underlying mechanism.

2. Material and Methods

2.1. Reagents. All solutions were prepared in ultrapure water (MilliQ). Pb(II) solution was obtained from dilution of a certified standard (0.100 M Metrohm). The ionic strength is set with $NaNO_3$ (Fluka, trace select). Stock solutions of MES (2-(*N*-morpholino)ethanesulfonic acid) buffers were prepared from the solids (Fluka, Microselect, >99.5%). Diluted HNO_3 solutions (Merck suprapure) were used to adjust the pH.

Carboxymethyldextran (CMD) was prepared from dextran produced by bacteria of the species *Leuconostoc mesenteroides*. This neutral polysaccharide was obtained from Amersham Biosciences (Uppsala, Sweden). CMD macromolecules were obtained after chemical modification of two commercially available precursors, a low mass (unmodified) dextran denoted

* Corresponding author; E-mail: elise.rotureau@wur.nl, Tel.: +31-317-483066, Fax: +31-317-483777.

10.1021/jp800472g CCC: $40.75
Published on Web 07/11/2008

TABLE 1: Characteristic Parameters of the Different Synthesized Carboxymethyldextran Macromolecules: Number-Average Molecular Weight $\bar{M}_n$, Maximum Space Charge Density Γ^0_{max}/F, Degree of Substitution d_S, Mean Diffusion Coefficient and Mean Hydrodynamic Radius As Evaluated from Diffusion Coefficient Data at $I > 10$ mM $NaNO_3$ and the Stokes−Einstein Equation

polymer	$\bar{M}_n$[a]	Γ^0_{max}/F[b] (mM)	d_S[b] (%)	D_{CMD}[c] (m^2 s^{-1})	δ_{Hexp}[c] (nm)
T40	29 000	0	0	4.9×10^{-11}	5
T500	370 000	0	0	1.4×10^{-11}	17.5
$CMD^{26\%}_{T40}$	33 400	−88.5	26	4.0×10^{-11}	6.05
$CMD^{15\%}_{T500}$	410 000	−11.7	15	1.1×10^{-11}	23.0
$CMD^{37\%}_{T500}$	460 000	−16.2	37	8.9×10^{-12}	28.0

[a] Obtained by SEC-MALLS. [b] Obtained by potentiometric titration. [c] Obtained by DLS.

SCHEME 1: Chemical Structure of Synthesized Carboxymethyldextran Macromolecule[a]

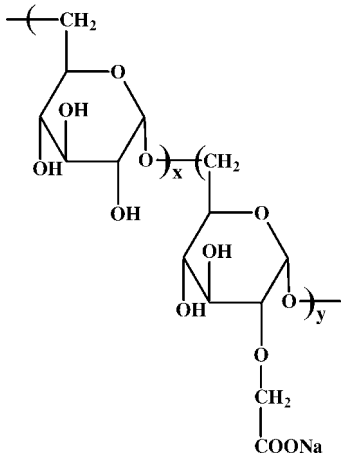

[a] Note that this scheme does not imply that the same hydroxyl group is substituted within all the glucopyranose units.

as T40 and a larger one indicated by T500. The molar masses and polydispersity indexes of T40 and T500 were determined by size exclusion chromatography coupled to multiangle laser light chromatography (SEC-MALLS) and the corresponding results are reported in Table 1. CMD was obtained and then purified following the synthetic route given by Mauzac and Jozefonvicz[21] and Chaubet et al.[22] It comprises a step-by-step carboxymethylation of dextran (denoted as $Dex(OH)_3$) according to the reaction scheme:

$$[Dex(OH)_3]_{x+y} \xrightarrow[(2)\ ClCH_2COOH,\ H_2O,\ 60\ °C]{(1)\ NaOH,\ H_2O,\ 0\ °C} [Dex(OH)_3]_x[Dex(OH)_2(OCH_2COONa)]_y \quad (1)$$

where the stoichiometric parameters x and y correspond to those indicated in Scheme 1. The overall yield was approximately 80%. The degree of substitution, denoted as d_S, indicates the fraction of carboxylated glucosidic groups. The magnitude of d_S is controlled by the number of successive carboxymethylation reactions performed. The hydroxyl groups located at C2 positions within the glucopyranose units chain are mostly substituted, but multiple substitution within a given monomer unit is not excluded.[23] Resulting d_S values (or, equivalently, the carboxylate densities) were determined after careful protolytic titration. Three different CMD varieties were prepared with differences in d_S and molar mass and these will be denoted as $CMD^{26\%}_{T40}$, $CMD^{15\%}_{T500}$, and $CMD^{37\%}_{T500}$. The subscripts and superscripts in the notation refer to the molecular precursor used as a reactant in (1) and the percentage of substitution in the synthesized CMD, respectively. The values of the charge density and molar mass as determined by size exclusion chromatography coupled to a multi-angle laser light scattering are detailed in Table 1. Polysaccharide solutions were prepared with filtered (0.22 μm) Milli-Q water 24 h prior to experiments and subsequently stored at 4 °C. Protolytic titrations were performed previously[20] to determine the degree of deprotonation as a function of pH and ionic strength (10 and 100 mM). To study metal speciation, SCP measurements were performed at pH 6.2 using MES buffer. Under these conditions, essentially all carboxylic groups are deprotonated implying that the volume charge densities of each CMD are given as in Table 1.

2.2. Apparatus. An Ecochemie Autolab type II potentiostat was used in conjunction with a Metrohm 663VA stand. The electrometer input impedance of this instrument is larger than 100 GΩ. The working electrode was a Metrohm multimode mercury drop electrode (surface area 4.0×10^{-7} m^2, Merck mercury, p.a.). The auxiliary electrode was glassy carbon and the reference electrode was a calomel electrode encased in a 0.1 M KNO_3 salt bridge. The glass wall of the cells used in these experiments is coated with a polystyrene film to reduce trace metal adsorption by cell walls.[24]

2.3. Measurement Procedure. The technique of depletive stripping chronopotentiometry (SCP) consists of a deposition step followed by a quantification step where the accumulated metal is reoxidised by application of a constant current. The analytical signal (the stripping time or transition time, τ) is a measure of the accumulated metal that is directly correlated with the pertinent species concentration in solution. After the accumulation step at the specified deposition potential E_d, a stripping current, I_S, of 1×10^{-9} A was applied in quiescent solution until the potential reached a value well past the reoxidation transition plateau. The magnitude of I_S is low enough to warrant complete depletion ($I_S\tau$ constant). The primary signal is the change of potential with time which is automatically converted into the dt/dE versus E format. The area under dt/dE peak equals the transition time τ. The experiments were run as follows. A solution is made from 20 mL of pure water, 5 μL of HNO_3 and 2.2 mL of 1 M $NaNO_3$ and left under argon bubbling during 2 h to remove oxygen. Ample degassing is necessary to get a constant SCP signal; an argon blanket is maintained during measurements. The metal is then added in the form of $Pb(NO_3)_2$ and a reference measurement is performed, yielding the metal-only signal, τ_M. Together with a given quantity of CMD solution, 200 μL of buffer (MES: 2-(*N*-morpholino)ethanesulfonic acid)) is added to maintain the pH at 6.1. Metal-to-ligand ratios R ($=c_{M,t}/c_{L,t}$, $c_{L,t}$ being the total (smeared-out) carboxylate concentration and $c_{M,t}$ the total metal concentration) were set to 0.03 with $c_{M,t}$ fixed at 3×10^{-7} mol L^{-1}. The progress of the metal complexation process is followed by the measurement of the SCP signal of the complex system, denoted as τ^*_{M+L}, as a function of equilibration time. The uncertainty in τ^*_{M+L}/τ^*_M is checked experimentally in three consecutives measurements and is found to be about 10% on average.

2.4. Dynamic Light Scattering. DLS was used for the determination of the diffusion coefficient of CMD in the presence of metal ions. The light source was a Lexel 450 mW (max) multiline width Ar laser ($\lambda = 514.5$ nm). Light scattering measurements were carried out with the dynamic compact goniometer system (ALV/DLS/SLS-5000), Langen, Germany using the ALV-5000/E/WIN software. The detection angle was 90°. The measurements were performed in a thermostated cell

at 295 K. Addition of metal into the measurement cell containing the CMD solution is performed by means of an automatic titrator. The ionic strength is 0.1 M, and the pH is fixed at 6.1 by means of addition of MES buffer.

3. Theoretical Section

Let us consider the scheme of a metal ion M that may associate with a ligand L to form dissolved, electroinactive complexes ML and ML_2. The free metal ion M can be reduced to the metal atom, M^0, at the interface of an electrode in contact with the solution:

$$\begin{array}{ccccc} M + L & \underset{k_{d,1}}{\overset{k_{a,1}}{\rightleftharpoons}} & ML + L & \underset{k_{d,2}}{\overset{k_{a,2}}{\rightleftharpoons}} & ML_2 \\ \Big\updownarrow ne^- & & & & \\ M^0 & & & & \end{array} \quad (2)$$

The supply of metal to the electrode surface is governed by the diffusional transport of M, ML and ML_2 and the interconversion between these species as governed by the rate constants $k_{a,n}$ and $k_{d,n}$ ($n = 1$ or 2).

On a time scale t, the system is dynamic or static if the rates for the 3D association/dissociation reactions are fast or slow, respectively:

$$k_{d,n}\,t,\ k'_{a,n}\,t \begin{cases} >>1 & \text{dynamic} \\ <<1 & \text{static} \end{cases} \quad (3)$$

with $n = 1$ or 2 and $k'_{a,n}$ defined for conditions of excess of ligand as

$$k'_{a,n} = k_{a,n} c_{L,t} \qquad \text{and} \qquad k'_{a,n}/k_{d,n} = K'_n = K_n c_{L,t} \quad (4)$$

where K_n is the stability constant of ML_n and $c_{L,t}$ is the total ligand concentration. Dynamic complexes fully maintain equilibrium in the bulk solution whereas, at the other extreme, static ones are unable to maintain/restore equilibrium to any significant extent. Dynamic complexes contribute to an overall metal flux to an extent depending on the relative magnitudes of their diffusive and kinetic fluxes, ranging from fully labile (diffusion control) to nonlabile (kinetic control).[7,25]

3.1. Speciation Analysis. In SCP with a spherical electrode, the limiting deposition current for labile complex systems is

$$I_d^* = nFA\bar{D}c_{M,t}^*\left(\frac{1}{\delta} + \frac{1}{r_0}\right) \quad (5)$$

where $\bar{D}$ is the mean diffusion coefficient of the contributing labile species in solution, $c_{M,t}^*$ is the sum of free and labile species concentrations in the bulk solution, n is the number of electrons involved in the metal ion reduction process, F is the Faraday constant, A is the electrode area, δ is the diffusion layer thickness and r_0 is the radius of the electrode.

The mean diffusion coefficient is defined as

$$\bar{D} = \frac{c_M D_M + \sum_{i=1}^{n} c_{ML_i} D_{ML_i}}{c_{M,t}} \quad (6)$$

where the second term of the numerator encompasses the fully labile species and $D_M$and D_{ML_n} are the diffusion coefficients of the metal and of labile complexes ML_n, respectively. For macromolecular multisite ligands and low metal-to-ligand ratio, D_{ML_n} can be assumed to be equal to the diffusion coefficient of the macromolecule itself (unless M bridges two different macromolecules). For a system with labile complexes and $D_M \neq D_{ML_n}$, the diffusion layer thickness δ, is generally given by[26]

$$\delta = \gamma \bar{D}^{\alpha} \quad (7)$$

where γ is a constant coefficient and α is a parameter related to the hydrodynamic nature of the mass transport in the system. For a macroscopic electrode in a stirred system,[26] α generally assumes a value between $^1/_2$ (pure diffusion conditions) and $^1/_3$ (laminar flow) depending on the hydrodynamic conditions during the pre-electrolysis. Here the value is set to $^1/_3$ according to ref 27.

The limiting transition time, τ^*, is related to the total amount of metal accumulated during the deposition step for deposition potentials in the limiting current region of the metal/complex system, and proportional to the limiting deposition current I_d^*. For depletive SCP we then have[28]

$$\tau^* = \frac{I_d^* t_d}{I_S} \quad (8)$$

where t_d is the deposition time and I_S is the oxidizing strip current.

For labile systems:

$$\frac{\tau_{M+L}^*}{\tau_M^*} = \left(\frac{\bar{D}}{D_M}\right)^{(1-a)}\left(\frac{c_M + c_{ML}^{labile}}{c_{M,t}}\right) \quad (9)$$

The limiting transition time τ_{M+L}^* reflects the magnitude of the original flux irrespective of its nature (diffusion or kinetically controlled).[29] In the absence of kinetic contributions, the flux of species toward the electrode during the deposition step is determined by the labile metal species and the free metal. A decrease of τ^* as a function of equilibration time generally reflects a successive formation of complex species at a time scale much longer than that of the SCP technique.[29] As a consequence, these latter species are characterized by correspondingly low association/dissociation rate constants and are not SCP-labile.

3.2. Speciation Dynamics. For many metal complexes in aqueous medium, the rate of formation is described by the Eigen mechanism.[30,31] This mechanism comprises the rapid formation of an outer-sphere complex (ion pair) between the hydrated metal ion M and the ligand L, followed by the rate-limiting removal of water from the inner coordination sphere of the metal. For a divalent metal ion M^{2+} and a ligand L^- the scheme reads

$$M(H_2O)_6^{2+} + L^- \overset{K_{os}}{\rightleftharpoons} ML(H_2O)_6 \cdot L^+ \xrightarrow{k_w} ML(H_2O)_5^+ + H_2O \quad (10)$$

where the $\cdot$ denotes the ion pair. The overall rate constant of complex formation k_a is thus determined by k_w (rate constant of water substitution) and K_{os} (the stability constant for the intermediate outer-sphere complex). For successive complexes ML to ML_n, it reads

$$k_{a,n} = k_{w,n} K_{os,n} \quad (11)$$

expressing that each rate constant $k_{a,n}$ derives from the stability constant of the formation of the corresponding outer-sphere complex and the rate constant for release of the pertaining H_2O

molecule. The removal of a further water molecule is somewhat faster than that of the preceding one ($k_{w,n-1} > k_{w,n}$).[31]

For complexes with higher stoichiometry, ML_n ($n > 1$), the quantification of the overall interfacial flux of M requires consideration of the association/dissociation rates for all species ML to ML_n. For small and homogeneous ligands, the stepwise formation constant for ML is generally larger than that for ML_2 (i.e., $K_1 > K_2$).[31] Consequently, if in the system M/ML/ML_2 the equilibrium between M and ML is dynamic, then generally that between ML and ML_2 will often be dynamic as well.

Metal speciation and lability criteria will obviously depend on the nature and structure of the ligand and its physicochemical properties in solution. In the present study, we investigate carboxymethyldextran (CMD) as a soft colloidal ligand for Pb(II) ions. This polysaccharide has been previously characterized in terms of electrostatic and hydrodynamic properties[20] using a model recently developed by Duval et al.[32] In brief, neutral dextran macromolecules are known to possess sufficient internal flexibility to adopt a random coil structure. This is generally the case for polysaccharides with 1−6 linkages where the main origin of the elasticity is due to the twist of the C5−C6 bond.[33] Electrophoretic characterization and size analysis in the dilute regime have revealed a certain extent of hydrodynamic permeability and capability of changing in conformation (chain stretching and electrostatic swelling). At sufficiently high ionic strength ($I > 10$ mM), where long-range electrostatic effects are small, the CMD particle adopts a compact spherical form in which the polymer segments are essentially homogeneously distributed within the particle volume. Table 1 collects the hydrodynamic radii and the maximum volume concentrations of charges (Γ^0_{max}/F) that have been determined previously (see ref 20 for more details) for the three types of CMD. As a result of the soft nature of the polymer, interaction with metal ions may be expected to lead to complexes with one or more carboxylate sites.

4. Results and Discussion

4.1. Effect of Metal Complexation on Particle Size. The diffusion coefficients of the Pb(II)/CMD complexes were measured by dynamic light scattering to track possible changes in size variation that may occur upon metal binding, and to apply these values in the interpretation of SCP data. In metal-free solution at $I > 10$ mM and pH around 6, the CMD particle may be regarded as a random coil with a spherical geometry.[20] At the given level of ionic strength where electrostatic effects play a minor role, its conformational structure is governed by the balance between polymer/solvent mixing and the chain elasticity components.[20] Below CMD concentrations of 10 mg L^{-1}, the CMD suspension is in the dilute regime where the polymer concentration is much lower than the overlap concentration. Rheological data for unmodified neutral T500 and T40 dextran solutions show that the dilute regimes are attained for concentrations below 30 and 60 g L^{-1}, respectively.[34]

Let us first consider the case of $CMD^{37\%}_{T500}$ for which the binding of Pb(II) is most marked, as shown in Figure 1. For the range of metal-to-ligand ratios below 0.15, the diffusion coefficient of the colloidal complex remains equal to that of free CMD and no dependence with time is observed. For R above 0.15, we notice an increase of D_{M+L}, which is most likely due to the shrinking of the particle resulting from intramolecular binding of metallic ions as it is usually the case for water-soluble polyelectrolytes.[35,36] This finding indicates either a reduction of electrostatic swelling or an intramolecular complexation. Both effects induce a more compact macromolecular structure.

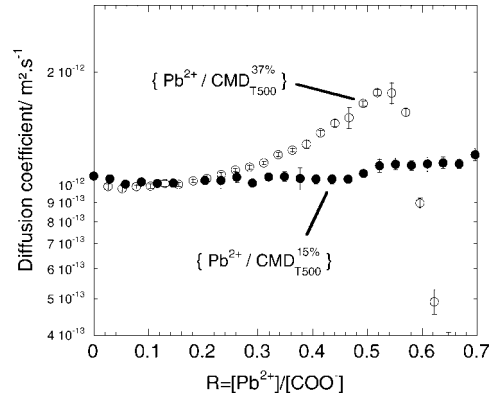

Figure 1. Diffusion coefficient of $CMD^{15\%}_{T500}$ and $CMD^{37\%}_{T500}$ as the function of the concentration ratio R= [Pb]/[COO^-] at pH = 6.1, I = 100 mM and T = 22 °C. The concentration of CMD is around 2 g L^{-1}.

Nevertheless, such shrinking is not significant for R lower than 0.15. The variation in size is much more pronounced for $CMD^{37\%}_{T500}$ as compared to $CMD^{15\%}_{T500}$, which is coherent with their respective volumic charge densities. The size decrease of $CMD^{37\%}_{T500}$ continues with increasing metal-to-ligand ratio until aggregation sets in at R around 0.5. This aggregation is provoked by the interparticle bridging by the coordinating Pb ions, leading to larger gel-like particles. Presumably, ML_2 is predominantly formed and, as a consequence, the aggregation is also driven by the overall neutralization of the colloidal complex at R = 0.5.

Only at increased polymer concentrations was it possible to obtain good quality data for the smallest and more dense CMD, i.e., $CMD^{26\%}_{T40}$. The size of this dextran with a radius of 6 nm at 0.1 M ionic strength is close to the detection limit of the DLS apparatus. Still, at a concentration of 4 g L^{-1}, an aggregation effect was observed for low R (≈0.05). The effect is not surprising because for this highly charged CMD the screening of charge at I = 100 mM is incomplete[20] and the intra- and interparticular metal binding is thus electrostatically strengthened. To avoid the domain of interparticular interactions, SCP analysis (section 4.2) is carried out at much lower polymer concentrations of 10^{-2} g L^{-1}.

4.2. Kinetics of Pb(II)/CMD Complexation. ***4.2.1. Complex Formation.*** To accurately follow the time dependence of the complexation of CMD with Pb(II), we measured the value of the limiting SCP transition time, τ^*_{M+L}, at a sufficiently low and constant E_d. Figure 2 presents a typical set of curves for the complex formation curves kinetics of the three different types of CMD.

The kinetics can be globally described by two stages: a rapid initial decrease of the signal within the first 600 s (time of the first measured point), followed by a gradual decrease over roughly the next 5−10 h. The time pattern could indicate the slow formation of additional metal complex species with strong differences in their dynamic nature as compared to the initially formed species. For latex nanoparticles covered by carboxylic groups ("hard" particles), no such kinetic features were observed on the time scale of the experiment, implying that the eventual equilibrium was rapidly established.[13] The time characteristics for Pb/CMD complex formation were found to vary with experimental conditions (ionic strength, R, CMD or nature of the metal) and these latter effects will be the subject of following articles. In the present exploratory study, we focus on conditions where (i) CMD carboxylate ligands are well in excess over the metal Pb(II) (R = 0.03), (ii) all carboxylate groups are

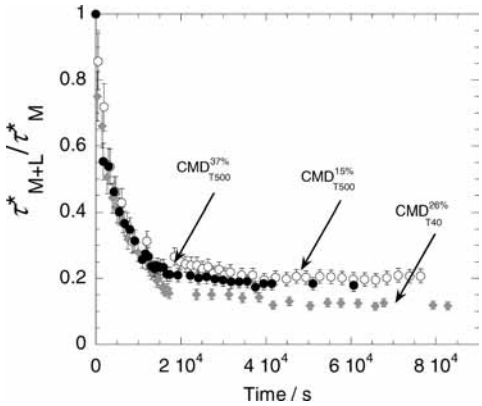

Figure 2. Variation of the normalized limiting transition time as a function of time at $E_d = -0.5$ V (case of $CMD^{26\%}_{T40}$, $CMD^{15\%}_{T500}$ and $CMD^{37\%}_{T500}$) with lead for a ratio $[Pb^{2+}]/[COO^-] = 0.03$, at the same conditions described for Table 2.

TABLE 2: Values of Constants Obtained by Means of the Fit of Experimental Data Using Eq 18, for the Three CMD with $K_{ML} = c_{ML}/(c_M c_L)$ Expressed in L mol^{-1} and $K_{M(LL)} = c_{M(LL)}/c_{ML}$ the Stability Constants of ML and M(LL), Respectively, $k_{a,1-1}$ and $k_{d,1-1}$ the Association and Dissociation Rate Constant Leading to M(LL) and k_{conf} the Rate Constant of the Conformation Step[a]

polymer	log K_{ML}	log $K_{M(LL)}$	$k_{a,1-1}$ (s^{-1})	$k_{d,1-1}$ (s^{-1})	k_{conf} (s^{-1})
$CMD^{26\%}_{T40}$	4.7 ± 0.1	1.3 ± 0.1	1.5×10^{-4}	2.7×10^{-5}	1.6×10^{-4}
$CMD^{15\%}_{T500}$	4.6 ± 0.1	0.9 ± 0.1	1.0×10^{-4}	3.7×10^{-5}	1.2×10^{-4}
$CMD^{37\%}_{T500}$	4.7 ± 0.1	0.9 ± 0.1	1.1×10^{-4}	3.8×10^{-5}	1.4×10^{-4}

[a] The experiments are performed at pH = 6.1−6.2, $I = 100$ mM and room temperature. The total concentration of lead is 3×10^{-7} mol L^{-1} and the concentration of carboxylate 1×10^{-5} mol L^{-1}.

deprotonated (pH = 6.0−6.2) and (iii) long-range electrostatic effects are negligible ($I = 100$ mM). For these conditions, the electrohydrodynamic properties of CMD in metal-free solution are well-known.[20]

4.2.2. Mechanism of M(LL) Formation. For the formation of the 1:1 lead monocarboxylate species in the CMD dispersion, the complexation is expected to be of the Eigen type with correspondingly fast kinetics.[31] To illustrate this, we compute $k_{a,1}$ from eq 11 with $k_w = 7 \times 10^9$ s^{-1} for Pb(II) and log $K_{os} = 0.31$ (in L mol^{-1})[31] leading to a value of 1.4×10^{10} L mol^{-1} s^{-1}. So, the formation of the $[Pb-OOC\equiv]^+$ complex (with $\equiv$ denoting the attachment to the polysaccharide structure) would be a fast process, comparable to Pb(II) complexation with monomeric carboxylic acids or similar oligosaccharides. The experimental data confirm this: $[Pb-OOC\equiv]^+$ formation is fast compared to the time scale of observation and consequently the apparent instantaneous reduction in τ^*_{M+L} comprises the formation of these 1:1 complexes. In addition, the full wave characteristics of the SCP response (with an effective measurement time scale on the order of seconds) after 10 min equilibration time, demonstrate the lability of ML species.[13,29] The soft permeable CMD entity contains around 99% (in mass) of water and hence the diffusion of free Pb_{aq}^{2+} ions can be considered equally fast inside and outside the particle. Consequently, the diffusion of free Pb^{2+} ions within the particle is fast on the time scale of the observed slow step in the complexation process. It might be argued that for a colloidal ligand dispersion the effective association and dissociation rate constants can differ from those for a homogeneous ligand solution.[10] Indeed, for the binding of Pb(II) by "hard" carboxylated latex particles, the association rate constants were found to be to 1 or 2 orders of magnitude lower than the Eigen derived values.[31] Moreover, in certain cases, the rate of formation of the outer-sphere complex might also be slowed down and even become the rate-limiting step.[37] However, even such colloidal complex formation rates remain far too fast to explain the observed time dependence for the present slow step in the Pb(II)/CMD complex formation. As a consequence, we have to postulate the formation of multidentate complexes in such a way that *additional* binding of Pb(II) occurs. For identical and independent ligands L,[38] Eigen predicts ML_2 formation to be even faster than ML formation ($k_{a,1} > k_{a,2}$). It therefore has to be concluded that the observed slow kinetics are bound to be due to properties of the CMD itself. More than one carboxylic group from one and the same chain has to be involved and apparently the complexation requires an appropriate conformational adjustment (see section 4.1). This preceding conformational step appears to be so slow that it governs the rate of complex formation. Then the rate-limiting step is no longer the removal of a water molecule (like in Eigen) but rather the preceding formation of the intermediate outer-sphere complex. This has the consequence that the rate of formation of this precursor complex would not be governed by the electrostatic Pb^{2+}/COO^- interaction (as expressed by K_{os}).[31] Instead, the formation would be controlled by the probability of bringing together two ligand sites from one and the same polymer chain.

Thus, for the reaction ML + L ⇆ M(LL) we would have

$$ML(H_2O)_5^+ + L^- \xrightarrow{k_{conf}} ML(H_2O)_5 \cdot L \overset{K_{ex}}{\rightleftharpoons} M(LL)(H_2O)_4 + H_2O \quad (12)$$

where (LL) denotes the coupling of two carboxylate ligands from the same CMD macromolecule and K_{ex} is the stability constant of the inner-sphere H_2O-L ligand exchange equilibrium.

K_{ex} can be straightforwardly related to the stability of the inner-sphere M(LL) complex, $K_{M(LL)} = c_{M(LL)}/c_{ML}$, and the stability constant of the outer-sphere complex ML·L, $K_{os,2} = c_{ML\cdot L}/c_{ML}$:

$$K_{ex} \equiv \frac{K_{M(LL)}}{K_{os,2}} \quad (13)$$

4.2.3. M(LL) Formation Kinetics. The overall rate constant for M(LL) formation, $k_{a,1-1}$, is determined by the rate constant for precursor formation (k_{conf}) together with the equilibrium distribution between $ML(H_2O)_5 \cdot L$ and $M(LL)(H_2O)_4$, as given by K_{ex}, and can be written as

$$k_{a,1-1} = k_{conf} \frac{K_{ex}}{1 + K_{ex}} \quad (14)$$

This rate constant, $k_{a,1-1}$, defines the rate of formation of M(LL):

$$R_{a,1-1} = k_{a,1-1} c_{ML} \quad (15a)$$

Because the 1:1 complex ML is in continuous equilibrium with free M, $R_{a,1-1}$ can also be written as

$$R_{a,1-1} = \frac{k_{a,1-1}}{1 + \frac{1}{K'_1}} (c_M + c_{ML}) \quad (15b)$$

The expression for $k_{a,1-1}$ which incorporates k_{conf}, does not contain the ligand concentration because the conformational step corresponds to an intramolecular process occurring on one and the same macromolecule between $[Pb-OOC\equiv]^+$ and another approaching $^-OOC\equiv$. In fact, the two ligands involved are

neither totally independent nor totally dependent species. In the present intramolecular case of $[Pb-OOC\equiv]^+$ and $\equiv COO^-$, the freedom of the second ligand appears to be strongly limited: its free, unrestricted diffusion to the location of $[PbOOC\equiv]^+$ would be realized on the submicrosecond time scale.[39] The effective limiting process, however, occurs on the time scale of hours and has to be related to the conformational constraints of the particular macromolecule involved. Moreover, it is bound to be energetically attractive to bring one $\equiv COO^-$ ligand to the site of $[Pb\text{-}OOC\equiv]^+$ because the formation of $[\equiv COO-Pb-OOC\equiv]$ implies loss of entropy for the macromolecule entity.

To sum up, the overall formation reaction of M(LL) is proposed to be as follows:

$$M + L \overset{K_{ML}}{\rightleftarrows} ML \overset{k_{conf}}{\rightarrow} M(LL) \qquad (16)$$

As explained above, the 1:1 Pb/carboxylate species (ML) are fully labile whereas M(LL) and possibly higher-order species, if any, would remain nonlabile or inert on time scales far beyond that of formation of ML (i.e., nonparticipating to the overall SCP deposition flux).

The initial part of the complex formation curve shows a fast decrease of the signal (see Figure 2) and is attributed to the ML formation. Once the equilibrium between M and ML is established, the slow formation of M(LL) is the only remaining process. The M(LL) concentration variation with time is directly obtained from the experimental data τ^*_{M+L}/τ^*_M.

The overall equilibration between M(LL) and ML + L (see reaction scheme (16)) is defined by the association of ML with another L and the back-reaction, i.e., the dissociation of M(LL). Using (15b), the corresponding rate equation can be written as

$$\frac{dc_{M(LL)}}{dt} = \frac{k_{a,1-1}}{1 + \frac{1}{K'_{ML}}}(c_M + c_{ML}) - k_{d,1-1}c_{M(LL)} \qquad (17)$$

Integration leads to an exponential variation of $c_{M(LL)}$ as a function of time:

$$c_{M(LL)}(t) = c^{eq}_{M(LL)}(1 - \exp(-k_{app}t)) \qquad (18)$$

where $c_{M(LL)}$ is the concentration of M(LL), $c^{eq}_{M(LL)}$ the concentration of M(LL) at equilibrium and k_{app} the apparent M(LL) formation rate constant as following from the integration of (17):

$$k_{app} = \frac{k_{a,1-1}}{1 + \frac{1}{K'_{ML}}} + k_{d,1-1} \qquad (19)$$

K_{ML} is the first parameter that is used to fit experimental data τ^*_{M+L}/τ^*_M. This constant determines the intercept point of the fitting curve as when $t \rightarrow 0$, $c_{M(LL)} \rightarrow 0$ and $\tau^*_{M+L}/\tau^*_M \rightarrow (\bar{D}/D_M)^{(1-\alpha)}$ with $\bar{D}$ incorporating K_{ML}. Indeed, according to eq 6, $\bar{D}$ depends on (i) the ratio of the labile species concentrations, i.e., c_{ML} and the free metal concentration c_M, and (ii) the total concentration of species participating to the flux, i.e., c_M and c_{ML}. The value of $\bar{D}$ remains constant and is directly obtained from K_{ML}, the diffusion coefficients of CMD (see D_{ML} values in Table 1) and D_{Pb} equal 9.85×10^{-10} m^2 s^{-1}. From K_{ML}, eq 9 and the total metal balance, c_M, c_{ML} and $c_{M(LL)}$ are retrieved (see Figure 3). The slow decrease of τ^*_{M+L}/τ^*_M is then attributed to the decrease of the second factor in the right-hand side of eq 9 due to the formation of nonlabile M(LL) species. Equation 18 provides a successful fit of the curve for $c_{M(LL)}$ as a function of time (see Figure 3) and experimental time dependence of ratios τ^*_{M+L}/τ^*_M (see Figure 4a,b). The parameters values resulting from these fittings are given in Table 2.

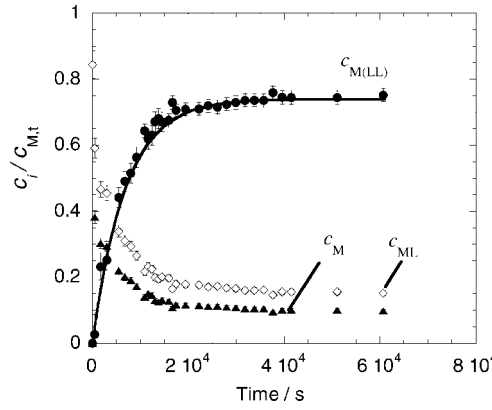

Figure 3. Variation of the concentrations c_M, c_{ML}, $c_{M(LL)}$ normalized by the total concentration of lead as a function of time, issue from experimental data of $CMD^{37\%}_{T500}$. The line indicates the fit obtained from eq 18 with log K_{ML}= 4.7, log $K_{M(LL)}$ = 0.9, $k_{conf} = 1.4 \times 10^{-4}$ s^{-1}.

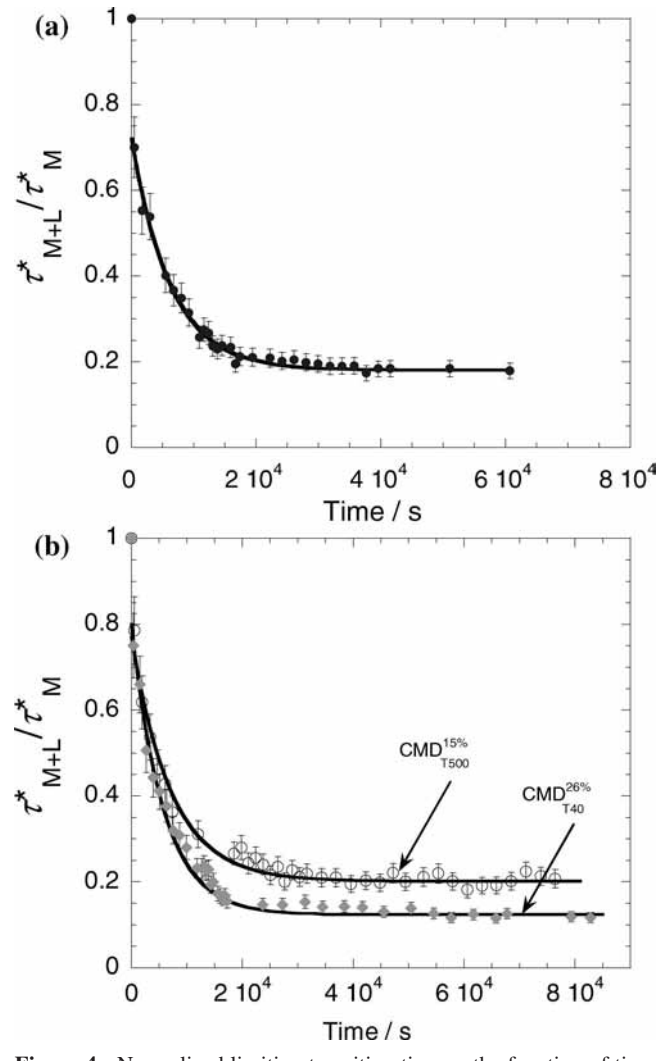

Figure 4. Normalized limiting transition time as the function of time in case of (a) $CMD^{37\%}_{T500}$ with the experimental data (black points) and the fit (line) corresponding to log K_{ML} = 4.7, log $K_{M(LL)}$ = 0.9, $k_{conf} = 1.4 \times 10^{-4}$ s^{-1} and in case of (b) $CMD^{26\%}_{T40}$ (diamonds) and $CMD^{15\%}_{T500}$ (circles) and the fits (lines) corresponding to log K_{ML} = 4.7, log $K_{M(LL)}$ = 1.3 and $k_{conf} = 1.6 \times 10^{-4}$ s^{-1} for $CMD^{26\%}_{T40}$ and log K_{ML} = 4.6, log $K_{M(LL)}$ = 0.9 and $k_{conf} = 1.2 \times 10^{-4}$ s^{-1} for $CMD^{15\%}_{T500}$. All K_{ML} stability constants are given in L mol^{-1}.

For the Pb(II)/CMD complexes studied here, the values for the log of the apparent stability constant K_{ML} (in L mol^{-1}) are

found to be around 4.7. It corresponds to a relatively weak complexation between carboxylates and Pb(II) under conditions where polyelectrolytic effects are reduced by the high ionic strength. Comparable orders of magnitude of K_{ML} are found, e.g., for Pb/partially esterified poly(methacrylic acid).[40] Figure 3 shows the concentration variation of M, ML and M(LL) as a function of time and clearly illustrates that M(LL) becomes the predominant species at equilibrium ($K_{M(LL)} = c_{M(LL)}/c_{ML} = 8$). Moreover, M(LL) appears to be stabilized as compared to ML by the particular spatial configuration of the complex with the two ligands attached to a single chain, commonly called the chelate effect. Comparable processes have been noted for the pectin−Cu complex for which the Cu(LL) formation is stabilized by a conformational change toward a more fibrillar structure,[17] and for the alginate−Pb complex with a special type of structured arrangement.[41] Furthermore, in our case, long-range electrostatic contribution does not play a major role in the M(LL) formation because the ionic strength is high.

The values of the rate constants ($k_{a,1-1}$, $k_{d,1-1}$, k_{conf}) are given in Table 2. Because K_{ex} is modest, the order of magnitude of k_{conf} is close to that of $k_{a,1-1}$ and extremely small as compared to the one predicted by the inapplicable Eigen mechanism. The limiting step is assumed to represent the approach and the contact between a $\equiv COO^-$ and a $[Pb-OOC\equiv]^+$ on the same chain. Formation of the $[\equiv COO-Pb-OOC\equiv]$ complex requires a specific local chain fluctuation in the neighborhood of the monodentate complex site, and this obviously makes strong demands on the chain elasticity. Because dextran is a relatively flexible polymer, M(LL) formation would tend to comprise two nonadjacent ligands[42] that rather generate a kind of polymer cross-link. The particular case of a coordinating metal ion requires specific and more complex molecular conformation around the metal as is known, e.g., chitosan/Me^{2+} (helical structure [43]) or alginate/Ca^{2+} ("egg-box" model[44]). Apart from this, the sterical hindrance of glucosidic monomers may also limit the approach of a second ligand to a $[Pb-OOC\equiv]^+$.

Table 2 sums up the relevant stability constants (K_{ML} and $K_{M(LL)}$) corresponding to the best fit of the experimental kinetic data as a function of CMD type. In general, the stability constants for the three types of CMD are quite close. Only $CMD_{T40}^{26\%}$ has a slightly higher value of $K_{M(LL)}$. As mentioned before, this particular CMD has the larger volume charge density with electric potentials still significant up to the 100 mM ionic strength level. As a consequence, the screening of the charges is not complete and counterion binding less weak as compared to the two other types of CMD. The volume charge density does not influence too much the kinetics as the values of k_{conf} for the different CMD's are quite similar (see Table 2). Apparently, the electrostatic effects with $CMD_{T40}^{26\%}$ do not have significant influence on the M(LL) formation rate constant. At the given pH and ionic strength, the slow kinetics is apparently related to overall chain rearrangement, irrespective of the density of charge within the particle and the separation between the pertaining ligand sites. This finding provides evidence for the nonelectrostatic nature of the rate-limiting step in the M(LL) formation.

5. Conclusion

This study underlines the complex process of interaction between transition metal ions and a soft particle bearing carboxylate groups (CMD). By means of a pertinent stripping chronopotentiometric technique, we established the formation of various types of complexes of Pb(II) with CMD. The system undergoes loss of metal complex lability as a function of time concomitant with formation of species with higher order stoichiometry on a time scale of hours. Reconformation of the chain in forming an ion-pair precursor complex is the rate-limiting step of the complex formation reaction, which therefore does not obey the rules of the Eigen mechanism.

Future detailed studies will focus on the effect of ionic strength in a wide range, on the nature of the metal, and on the metal release characteristics of the slowly formed intramolecular complexes of type M(LL). The issue is essential for proper understanding of the metal speciation in aqueous media with various types of metal-binding soft colloidal particles.

Acknowledgment. We thank Dr. J. P. Pinheiro for helpful assistance with the stripping chronopotentiometry technique, and Pr. R. M. Town (University of Southern Danemark) for carefully checking the manuscript. This work was performed within the ECODIS project (Contract No. 518043): Dynamic Sensing of Chemical Pollution Disasters and Predictive Modelling of their Spread and Ecological Impact, supported by the European Commission under the Sixth Framework Programme, subpriority 6.3, Global change and Ecosystems Global Change.

References and Notes

(1) Filella, M. Colloidal Properties of submicron particles in natural waters. In *Environmental Colloids and Particles: Behaviour, separation and characterisation*; Wilkinson, K. J., Lead, J. R. Eds.; Wiley: New York, 2007; Vol. 10.
(2) Lead, J. R.; Wilkinson, K. J. *Environ. Chem.* **2006**, *3*, 159–171.
(3) Deiana, S.; Gessa, C.; Palma, A.; Premoli, A.; Senette, C. *Org. Geochem.* **2003**, *34* (5), 651–660.
(4) Le Cloirec, P.; Andres, Y.; Faur-Brasquet, C.; Gerente, C. *Rev. Environ. Sci. Bio/Technol.* **2004**, *2* (2−4), 177–192.
(5) Yun, Y.-S.; Volesky, B. *Environ. Sci. Technol.* **2003**, *37* (16), 3601–3608.
(6) Doucet, F. J.; Lead, J. R.; Santschi, P. H. Colloid-Trace Element Interactions in Aquatic Systems. In *Environmental Colloid and Particles;* Wilkinson, K. J., Lead, J. R., Eds.; IUPAC Series on Analytical and Physical Chemistry of Environmental Systems; Wiley: Chichester, U.K., 2007; Vol. 10, pp 95–157.
(7) Buffle, J. *Complexation Reactions in Aquatic Systems. an Analytical Approach*; Ellis Horwood: Chichester, U.K., 1988.
(8) Town, R. M.; van Leeuwen, H. P. *J. Phys. Chem. A*, in press.
(9) Mota, A. M.; Correia dos Santos, M. M. In *Metal Speciation and Bioavailability in Aquatic Systems*; Tessier, A., Turner, D., Eds.; IUPAC Series on Analytical and Physical Chemistry of Environmental Systems; Wiley: Chichester, U.K., 1995; Vol. 3, pp 205–258.
(10) Pinheiro, J. P.; Minor, M.; van Leeuwen, H. P. *Langmuir* **2005**, *21* (19), 8635–8642.
(11) Pinheiro, J. P.; Minor, M.; van Leeuwen, H. P. *J. Electroanal. Chem.* **2006**, *587*, 284–292.
(12) Pinheiro, J. P.; Domingos, R. F.; Minor, M.; van Leeuwen, H. P. *J. Electroanal. Chem.* **2006**, *596*, 57–64.
(13) Pinheiro, J. P.; van Leeuwen, H. P. *J. Electroanal. Chem.* **2004**, *570* (1), 69–75.
(14) Nadal, A. M.; Arino, C.; Esteban, M.; Casassas, E. *Electroanalysis* **1991**, *3* (4−5), 309–18.
(15) Arino, C.; Nadal, A. M.; Esteban, M.; Casassas, E. *Electroanalysis* **1992**, *4* (8), 757–64.
(16) Gimenez, M. D.; Arino, C.; Esteban, M. *Anal. Chim. Acta* **1995**, *310* (1), 121–9.
(17) Vilhena, C.; Goncalves, M. L.; Mota, A. M. *Electroanalysis* **2004**, *16* (24), 2065–2072.
(18) Milas, M.; Rinaudo, M. *Curr. Trends Polym. Sci.* **1997**, *2*, 47–67.
(19) Lamelas, C.; Avaltroni, F.; Benedetti, M.; Wilkinson, K. J.; Slaveykova, V. I. *Biomacromolecules* **2005**, *6* (5), 2756–2764.
(20) Rotureau, E.; Thomas, F.; Duval, J. F. L. *Langmuir* **2007**, *23* (16), 8460–8473.
(21) Mauzac, M.; Josefonvicz, J. *Biomaterials* **1984**, *5*, 301–304.
(22) Chaubet, F.; Champion, J.; Maïga, O.; Mauray, S.; Jozefonvicz, J. *Carbohydr. Polym.* **1995**, *28*, 145–152.
(23) Krentsel, L. B.; Ermakov, I. V.; Yashin, V. V.; Rebrov, A. I.; Litmanovich, A. D.; Plate, N. A.; Chaubet, F.; Champion, J.; Jozefonvicz, J. *Vysokomol. Soedin., Ser. A Ser. B* **1997**, *39* (1), 83–89.
(24) Pinheiro, J. P.; Bosker, W. *Anal. Bioanal. Chem.* **2004**, *380*, 964–968.
(25) van Leeuwen, H. P. *Electroanalysis* **2001**, *13* (10), 826–830.

(26) Levich, V. G. *Physicochemical Hydrodynamics*; Prentice Hall: Englewood Cliffs, NJ, 1962.

(27) Diaz-Cruz, J. M.; Arino, C.; Esteban, M.; Casassas, E. *J. Electroanal. Chem.* **1992**, *333*, 33–45.

(28) van Leeuwen, H. P.; Town, R. M. *J. Electroanal. Chem.* **2002**, *536*, 129–140.

(29) van Leeuwen, H. P.; Town, R. M. *J. Electroanal. Chem.* **2004**, *561*, 67–74.

(30) Eigen, M.; Wilkins, R. G. *Adv. Chem. Ser.* **1965**, *49*, 55–80.

(31) Morel, F. M. M.; Hering, J. G. *Principles and Applications of Aquatic Chemistry*; Wiley: New York, 1993.

(32) Duval, J. F. L.; Ohshima, H. *Langmuir* **2006**, *22*, 3533–3546.

(33) Rief, M.; Oesterhelt, F.; Heymann, B.; Gaub, H. E. *Science* **1997**, *275*, 1295–1297.

(34) Rotureau, E.; Durand, A.; Dellacherie, E. *Eur. Polym. J.* **2006**, *42*, 1086–1092.

(35) Sarraguça, J. M. G.; Pais, A. A. C. C. *Phys. Chem. Chem. Phys.* **2006**, *8*, 4233–4241.

(36) Takagi, S.; Tsumoto, K.; Yoshikawa, K. *J. Chem. Phys.* **2001**, *114*, 6942–6949.

(37) Buffle, J.; Zhang, Z.; Startchev, K. *Environ. Sci. Technol.* **2007**, *41*, 7609–7620.

(38) Salvador, J.; Puy, J.; Galceran, J.; Cecilia, J.; Town, R. M.; van Leeuwen, H. P. *J. Phys. Chem. B* **2006**, *110*, 891.

(39) Doucet, D.; A, R.; Hagen, S. J. *Biophys. J.* **2007**, *92*, 2281–2289.

(40) Cleven, R. F. M. J. Heavy metal/polyacid interaction: an electrochemical study of the binding of Cd(II), Pb(II) and Zn(II) to polycarboxylic and humic acids. Ph.D. thesis, Wageningen University, 1984.

(41) Fukushima, M.; Tatsumi, K.; Wada, S. *Anal. Sci.* **2001**, *17*, 663–666.

(42) Garces, J. L.; Mas, F.; Cecilia, J.; Galceran, J.; Salvador, J.; Puy, J. *Analyst* **1996**, *121*, 1855–1861.

(43) Webster, A.; Halling, M. D.; Grant, D. M. *Carbohydr. Res.* **2007**, *342*, 1189–1201.

(44) Rees, D. A. *Pure Appl. Chem.* **1981**, *53*, 1–14.

JP800472G